PHOTOINDUCED REFRACTIVE INDEX VARIATION IN THE KDP SINGLE CRYSTALS WITH INCORPORATED TiO$_2$ NANOPARTICLES UNDER CW LASER EXCITATION

V.YA. GAYVORONSKY,[1] M.A. KOPYLOVSKY,[1] V.O. YATSYNA,[1]
A.I. ROSTOTSKY,[1] M.S. BRODYN,[1] I.M. PRITULA[2]

[1]**Institute of Physics, Nat. Acad. of Sci. of Ukraine**
(46, Nauky Prosp., Kyiv 03680, Ukraine; e-mail: vlad@iop.kiev.ua)

[2]**STC "Institute for Single Crystals", Nat. Acad. of Sci. of Ukraine**
(60, Lenin Ave., Kharkiv 61001, Ukraine)

For the first time, the impact of TiO$_2$ (anatase modification) nanocrystals on the photoinduced optical absorption and refractive index variations in KDP single crystals with the self-action of CW laser radiation at 532 and 1064 nm is studied. It is shown that the incorporation of anatase nanoparticles changes the sign of the refractive nonlinear optical response relatively to that for the KDP crystal matrix at 532 nm due to the resonance overlapping of the energy states of intrinsic defects in the crystal matrix and the surface states of TiO$_2$ nanoparticles. The sign and the magnitude of the photoinduced variations depend on the concentration of incorporated nanoparticles, crystal growth sector, and irradiation wavelength.

1. Introduction

Single crystals (SCs) of potassium dihydrogen phosphate (KDP) draw the special attention due to their unique collection of properties: the wide range of a transparency, electrooptical and piezooptical effects, relatively high value of a second-order nonlinear susceptibility, and the possibility of growing the large-size crystals. They are among few materials widely used in industrial laser facilities as the frequency multipliers, parametric amplifiers, and electrooptical shutters.

Nowadays, the design of new nonlinear optical (NLO) materials based on the inorganic water-soluble matrices with the addition of organic and inorganic impurities [1–3] is urgent. The control of a variety of important characteristics gives rise to the applications of such systems as modeling objects in nonlinear optics, photonics, and optoelectronics. Adding the certain organic and inorganic impurities in KDP family crystals can improve the useful properties of materials and devices based on them [4–6].

The possibility of growing the KDP SCs with incorporated TiO$_2$ nanocrystals of the anatase modification has been shown recently [7]. The presence of anatase

nanoparticles (NPs) in the crystal matrix caused an enhancement of the cubic NLO response and a change of the sign of the nonlinear refraction index of the composite system at the excitation by picosecond pulses at 1064 nm. The effect has been explained by the resonant excitation of TiO$_2$ NPs surface defect states under the resonant picosecond laser irradiation [8].

The KDP SCs are widely used for the laser radiation frequency conversion in powerful laser setups. The basic phenomenon limiting their output power is the low laser-induced damage threshold [9]. Therefore, the understanding of its nature is important for the further improvement of functional properties of these systems. It is considered that the laser-induced damage threshold is determined by intrinsic KDP defects (not of the origin of impurities), which are formed at the stage of crystal growth or during the interaction of the laser radiation with a crystal. These defects have been identified by electron paramagnetic resonance and optical spectroscopy techniques as (i) interstitial hydrogen atom H^0; (ii) the A-radical – [HPO$_4$]$^-$, the hole polaron localized on the oxygen ion near the hydrogen vacancy; (iii) the B-radical – [H$_2$PO$_4$]^0, the autolocalized hole polaron; (iv) electron center (PO$_3$)$^{2-}$ based on the oxygen vacancy, and were studied in the nanosecond [10, 11] and femtosecond ranges of pulse duration [9, 12].

At room temperature, the transient absorption of KDP SCs in the 1.5–4.0-eV range with a maximum of about 2.3 eV is related to optical transitions between valence band (VB) states and local states corresponding to the hole center in the form of A- or B-radical [13]. Electron centers based on oxygen vacancies (PO$_3$)$^{2-}$ in the KDP crystals can be associated with the optical absorption band in the range of 1–2 μm [14]. The comparison of data obtained in nano- and femtosecond ranges confirms the participation of oxygen vacancies in the crystal laser-induced damage [9].

The self-action technique of continuous wave (CW) laser irradiation at 532- (2.33 eV) and 1064-nm (1.17 eV) wavelengths was used to study partial contributions of the KDP matrix intrinsic defects and the anatase NPs subsystems to the NLO response of the material and their interaction. Such approach has been approved for the investigation of organic dye aggregates in a liquid crystal matrix [15, 16]. In the following text, we will refer the laser excitation condition at 532 nm as resonant, because it corresponds to the resonant excitation of the KDP and the anatase VB electrons into A-/B-radicals states of the matrix and into a deep defect state of the NPs [17], respectively.

Laser quanta 1.17 eV (1064 nm) in energy can excite the oxygen vacancies in the KDP matrix [18] (the mechanism is insufficiently studied) and electrons trapped at the deep states in the gap of anatase. The energy is also enough to activate the migration of protons in the KDP matrix [13]. We suggest that the latter mechanism is the most important in the photoinduced variation of the refractive index under the CW laser excitation, because the volume fraction of NPs in the composite system does not exceed 6×10^{-5} %. The photoexcited electrons in NPs are trapping on their interfaces and can affect the matrix local hydrogen bonds network redistribution. The formation of electron centers (interstitial H^0) is possible due to redox reactions.

At room temperature, the thermostimulated migration of hole polarons and H^0-centers takes place. It is not accompanied with the charge carriers injection into the conduction or valence band. The slow components of transient photoinduced processes with characteristic relaxation times from tens of milliseconds to seconds are referred to the processes of tunnel recharging of defects or annihilation of hydrogen vacancies associated with impurity/structural defects [13], which are controlled by the diffusion transport of hydrogen atoms. Therefore, under the CW laser excitation, the anatase NPs can significantly affect the hydrogen bonding network and the mobility of defects in the KDP crystalline matrix, which results in the photoinduced changes of the refractive index.

2. Samples

Nominally pure KDP SCs and crystals with incorporated TiO_2 NPs were grown by the temperature reduction method [7]. The anatase NPs were obtained by the method of precipitation with subsequent microwave heating and calcination of the resultant powder [8]. The average dimension of anatase NPs determined from the

data of transmission electron microscopy and X-ray analysis was 15 nm. The concentration of NPs in the growth solution varied from 10^{-5} to 10^{-3} wt. %. Incorporation of TiO_2 NPs in the crystal matrix does not reduce significantly the growth rate.

X-ray analysis showed that TiO_2 NPs do not distort the structure of the $KDP:TiO_2$ SC, because, in the growth process of the crystals, NPs are pushed aside from the crystallization front, and then "captured" by the boundaries between growth layer stacks [8]. This leads to the formation of the 1D layered macroscopic structure ...$KDP:TiO_2:KDP$... with a spatial period of ~ 15–20 μm. The high optical quality of $KDP:TiO_2$ SCs was shown experimentally [19].

The experimental samples were cut from different crystal growth sectors in the form of thin $10 \times 10 \times 0.8$ mm^3 plates perpendicularly to the optical axis (Z-cuts) with faces oriented along the crystallographic axes. Therefore, two series of samples were used in the experiments: (a) those cut from pyramidal (P) growth sector {101} and (b) from prismatic (Pr) growth sector {010}. The anatase NPs incorporation layers are tilted to the optical axis in the P sector and parallel in the Pr one. It should be noted that the incorporation coefficient practically equals to 1 for the P sector, whereas it is two times less for the Pr one. Thus, the NPs impact on the NLO response of the composite system can differ significantly for the samples cut from different growth sectors.

The linear transmittance spectra for nominally pure and $KDP:TiO_2$ crystals are presented in Fig. 1. The transmission coefficients in the visible and near-IR ranges are determined by the interfaces reflection losses. In the UV range, the magnitude of transmittance for the P and Pr sectors are different due to the fact that the P samples contain less polyvalent impurities. It is worth noting the enhancement of the transmittance of the Pr-4 sample (10^{-4} wt. %) against the pure crystal Pr at about 270 nm (Fig. 1,b), which is comparable with that of the P one (Fig. 1,a). This takes place due to both the low NPs concentration for the efficient UV absorption and to the effective adsorption of the impurities (especially polyvalent metal atoms) at the developed NPs interface during the growth stage.

3. Experimental Setup

Self-action effects of continuous wave laser radiation in KDP SCs with incorporated TiO_2 NPs were characterized by analyzing a distortion of the angular convergence/divergence of the beam focused on the sample and a variation of the sample transmittance versus the

laser intensity. The experimental setup and the technique were described in [16]. The measurements were performed with CW diode-pumped laser sources at 532 nm (2.33 eV) and 1064 nm (1.17 eV) with Gaussian spatial beam profiles. The laser power was varied by up to 15 mW using a neutral attenuator, whose transmission was ranged between 1% and 50%. The characteristic diameters of laser beams on the samples were about 0.2/0.3 mm for 532/1064-nm laser sources, respectively, and did not change over the time of the experiment.

The variation of the sample transmittance versus the laser intensity I characterizes photoinduced changes of the optical absorption $\Delta\alpha = \beta I \sim \mathrm{Im}(\chi^{(3)})I$, where β is the efficient two-photon absorption coefficient, and $\chi^{(3)}$ is the cubic NLO susceptibility; $\mathrm{Im}(\chi^{(3)}) > 0$ and $\mathrm{Im}(\chi^{(3)}) < 0$ correspond, respectively, to the photoinduced darkening of the sample ($\Delta T < 0$) and to the photoinduced bleaching ($\Delta T > 0$). The total transmittance of the sample with account of the Gaussian spatial beam profile $T(I) = T_{\mathrm{lin}} \ln(1 + q)/q$ is defined by the linear (spectral) transmittance T_{lin} and the NLO one; $q(I) = \beta I L_{\mathrm{eff}}$ is a dimensionless parameter that is proportional to the laser intensity I, β, and the effective self-action length $L_{\mathrm{eff}} = (1 - \exp(-\alpha L))/\alpha$, where L is the sample length, and α is the optical absorption coefficient. Estimations of $\mathrm{Im}(\chi^{(3)})$) were performed by the approximation of the obtained experimental dependences with the $T(I)$ formula [17]. In order to study the optical absorption photoinduced changes precisely, the samples were positioned on a photodiode aperture in order to avoid the scattering losses. The distance between the lens and the sample was varied to change the laser beam diameter on the sample and therefore, the intensity range to operate.

The photoinduced variation of the refractive index of the samples is analyzed by changes of the transmittance through the diaphragm (so-called on-axis transmittance) in the far field versus the laser intensity. The samples were positioned after the beam waist. The positive refractive index variation ($\Delta n > 0$ – self-focusing effect) provides the focusing and the narrowing of the transmitted beam in the far field and an enhancement of the on-axis transmittance through the diaphragm. The negative variation ($\Delta n < 0$ – self-defocusing effect) causes an increase of the beam diameter and a reduction of the on-axis transmittance. The refractive index variation is proportional to the real part of the cubic NLO susceptibility $\Delta n = n_2 I \sim \mathrm{Re}(\chi^{(3)})I$. The technique of the estimation of parameters is described in [16]. The reversibility of the NLO response was checked by the consequent
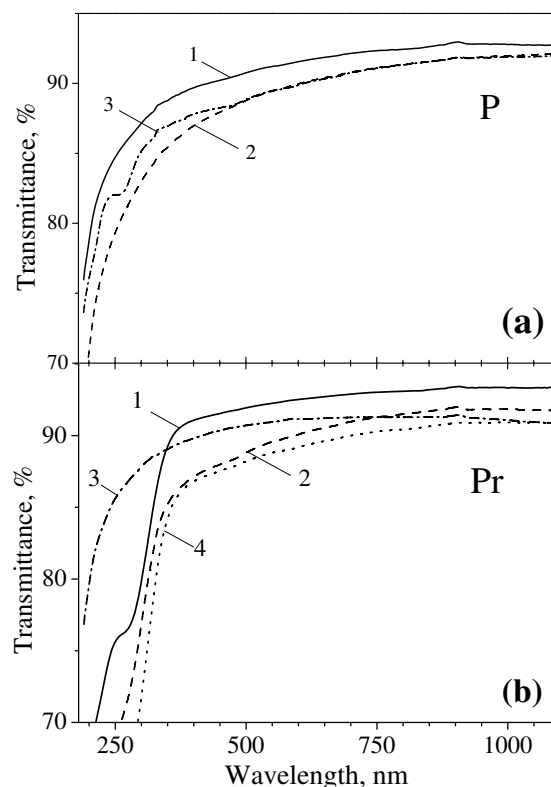

Fig. 1. Transmittance spectra of the pure KDP and KDP:TiO$_2$ crystals cut from pyramidal (*a*) P and prismatic (*b*) Pr growth sectors: *1* – nominally pure KDP; *2, 3* and *4* – KDP:TiO$_2$ with 10^{-5}, 10^{-4} and 10^{-3} wt.% of TiO$_2$ NPs in the growth solution

rise and the decrease of the laser power/intensity with an attenuator. The obtained dependences of the total and on-axis transmittances versus the laser intensity of the studied samples were reversible.

4. Experimental Results

The results of studies of the photoinduced transmittance variation ΔT in KDP SCs due to the self-action effects at 532 and 1064 nm are presented in Fig. 2. All dependences were normalized to the linear transmission coefficient of the samples obtained from the spectroscopic data (Fig. 1). At the 532-nm wavelength, the minor photoinduced bleaching ($< 0.5\ \%$) is observed in the investigated crystals from both growth sectors. At the 1064-nm wavelength, the photoinduced darkening is observed. Its magnitude is less in the Pr sector samples than that in the P ones. The effect depends on the concentration of incorporated TiO$_2$ NPs insignificantly.

The imaginary parts of the cubic NLO susceptibility $\mathrm{Im}(\chi^{(3)})$ estimated in the laser intensity range 5–
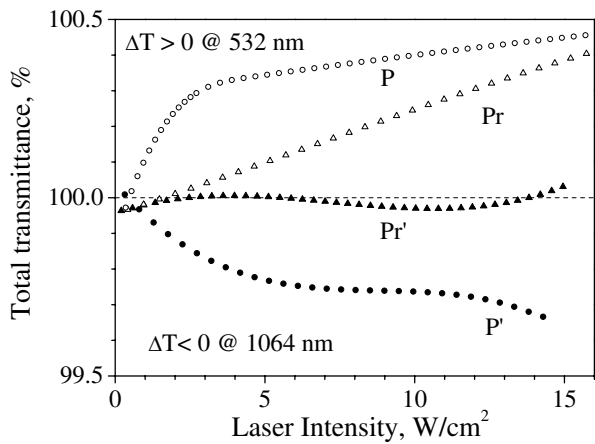
Fig. 2. Normalized total transmittance versus the laser intensity for nominally pure KDP single crystals from the pyramidal (circles) and prismatic (triangles) sectors at 532 (P and Pr) and 1064 (P' and Pr') nm

10 W/cm^2 are presented in Table. The symbolic notation of the samples given in the table is used in what follows. The magnitude of the bleaching effect at 532 nm increases with the concentration of anatase NPs for the P samples and slightly decreases for the Pr samples. At 1064 nm, the NPs incorporation slightly increases the Im($\chi^{(3)}$) for both growth sectors. The analysis of the total transmittance photoinduced changes shows that, in the investigated intensity range, the observed ΔT can be connected with the excitation and the relaxation of the matrix intrinsic defect states [13]. The negligible photoinduced darkening of the KDP crystals at 1064 nm can be associated with the excitation of the oxygen vacancies gap states and the proton migration activation effect.

The photoinduced variation of the on-axis transmittance in the far field due to the self-action of the CW laser radiation is presented in Fig. 3 for the SCs cut from the P sector. All dependences are normalized to the corresponding on-axis transmittance coefficient at the low-intensity range ($I < 1$ W/cm^2). The dependences for the KDP and KDP:TiO$_2$ crystals differ significantly. The self-focusing effect ($\Delta n > 0$) takes place for the P sample at 532 nm, which corresponds to the resonant excitation of the matrix intrinsic defects. The resonant excitation of the NPs surface defect states causes the interaction of photoinduced charge carriers at their interface with the H-bonding network and the refractive NLO response sign change. At a relatively low intensity, the self-focusing ($\Delta n > 0$) turns into the self-defocusing ($\Delta n < 0$) one. The last effect saturates, as the intensity
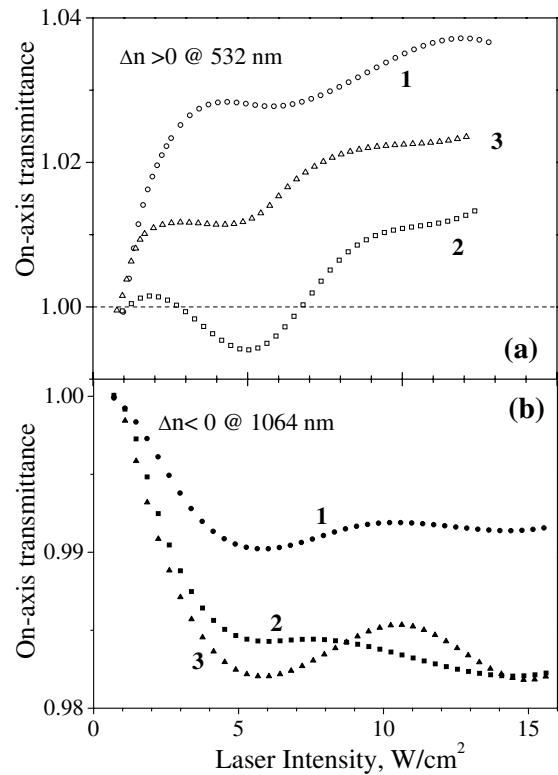

Fig. 3. Normalized on-axis transmittance in the far field versus the laser intensity at 532 (a) and 1064 (b) nm for the crystals cut from the pyramidal growth sector: P (1), P-5 (2) and P-4 (3). The sample notation is presented in Table

grows, and turns to the self-focusing regime, which is typical of the KDP crystal matrix. At 1064 nm, the beam self-defocusing is observed at relatively low intensities in the nominally pure P crystal. The anatase NPs incorporation causes the increase of the effect. The further increase of the laser radiation intensity results in the saturation of the self-defocusing effect.

The magnitudes of the real part of the cubic NLO susceptibility Re($\chi^{(3)}$) at $I < 5$ W/cm^2 and the photoinduced refractive index variation Δn at 3 W/cm^2 are presented in Table. The estimations were performed for the P and Pr sets on the basis of the on-axis transmittance dependences presented in Figs. 3 and 4.

For the P set, we can conclude the following. The refractive NLO response of the KDP SCs and the impact of anatase NPs on the Δn variation are significantly different in the case of the resonant excitation and at 1064 nm. However, in both cases, the NPs incorporation leads to a negative contribution to the on-axis transmittance changes of the samples. At the resonant excitation, the refractive NLO response sign

T a b l e. Imaginary and real parts of the cubic nonlinear optical susceptibility $\chi^{(3)}$ and photoinduced changes of the refractive index Δn at 532 and 1064 nm for the KDP and KDP:TiO$_2$ single crystals with various TiO$_2$ NPs concentrations in the growth solution cut from the pyramidal (P) and the prismatic (Pr) growth sectors

Growth sector	TiO$_2$ NPs, wt. %	Notation	532 nm			1064 nm		
			Im($\chi^{(3)}$), 10^{-7} esu	Re($\chi^{(3)}$), 10^{-4} esu	Δn, 10^{-5}	Im($\chi^{(3)}$), 10^{-7} esu	Re($\chi^{(3)}$), 10^{-4} esu	Δn, 10^{-5}
P	0	P	−1.6	10	6.9	1.6	−0.7	−0.5
	10^{-5}	P-5	−2.5	−1.7	−1.2	3.6	−1.3	−0.9
	10^{-4}	P-4	−5.3	−0.8	−0.6	2.6	−1.6	−1.1
Pr	0	Pr	−4.3	−1.5	−1.1	2.1	−1.7	−1.2
	10^{-5}	Pr-5	−3.5	5.3	3.6	2.7	−1.5	−1.1
	10^{-4}	Pr-4	−2.5	6.2	4.2	3.9	−1.3	−0.9
	10^{-3}	Pr-3	−2.4	3.7	2.6	4.5	−0.5	−0.4

changes in KDP:TiO$_2$ SCs relatively to the matrix one. At 1064 nm, only the magnitude of self-defocusing effect grows.

The normalized on-axis transmittance in the far field versus the laser intensity for the Pr series is presented in Fig. 4. One can see the drastic NLO response modification, as the NPs concentration in the matrix increases. For the resonant excitation at 532 nm, the minor self-defocusing $\Delta n < 0$ in the Pr sample in the initial intensity range turns into a substantial self-focusing effect with the incorporation of anatase NPs. The mentioned features are opposed to the corresponding ones in the P set response. The magnitude of self-focusing effect increases with the NPs concentration. With the further increase of the laser intensity, the effect saturates and turns into the self-defocusing typical of the KDP SC matrix.

At 1064 nm, the weak self-focusing of the beam in the initial intensity range saturates and turns into the effective self-defocusing in the Pr sample. For the KDP:TiO$_2$ SCs, the self-defocusing effect starts at lower radiation intensities, and its magnitude decreases with the rise of the anatase NPs concentration. The last feature is the most pronounced in the Pr-3 sample.

According to the data in Table, the incorporation of NPs into the P sector changes the sign and reduces the refractive NLO response at 532 nm by about one order. In the Pr sector, the self-defocusing in the crystal matrix (Pr: $\Delta n = -1.1 \times 10^{-5}$) is replaced by the self-focusing in the case of KDP:TiO$_2$ (Pr-4: 4×10^{-5}). The 532-nm irradiation causes the resonant excitation both of the KDP matrix and the anatase NPs intrinsic defect states. Therefore, the incorporation of TiO$_2$ NPs effectively changes the refractive NLO response of the composite system. At 1064 nm for the P sector, the effect of self-defocusing in the matrix (P: -0.5×10^{-5}) increases
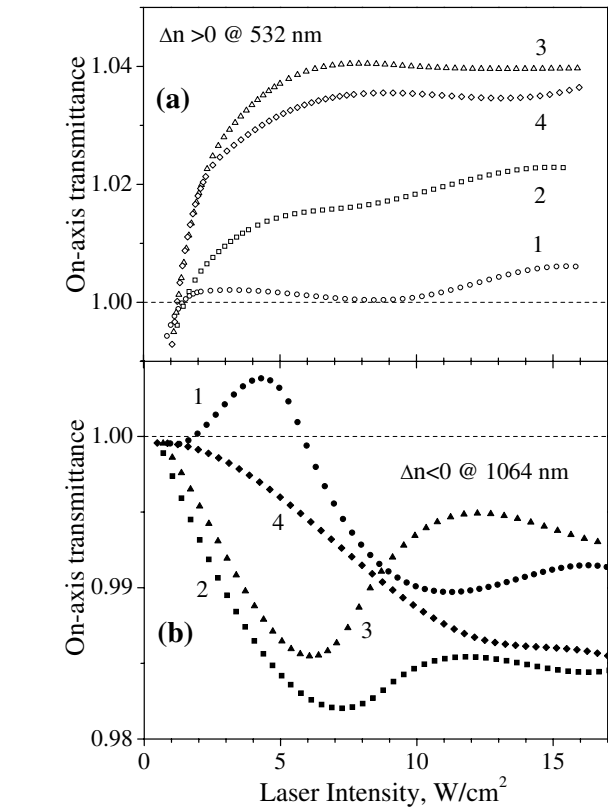

Fig. 4. Normalized on-axis transmittance in the far field versus the laser intensity at 532 (a) and 1064 (b) nm for the crystals cut from the prismatic growth sector: Pr (1), Pr-5 (2), Pr-4 (3) and Pr-3 (4). The sample notation is presented in Table

twice with the NPs incorporation (P-4: -1.1×10^{-5}). On the contrary, in the Pr sector, the incorporated NPs reduce the self-defocusing effect in the KDP matrix.

The comparison of the photoinduced variations of the refractive index/absorption (Re($\chi^{(3)}$)/Im($\chi^{(3)}$)) reveals

the prevalence by three orders of magnitude of the refractive contribution versus the absorptive one. This means the following: the weak photoinduced absorption of intrinsic defects of the crystalline matrix and anatase NPs subsystems causes the essential non-local charges redistribution in the composite system. Due to a high mobility of protons, we can conclude that the efficient photoinduced refractive response is defined by a perturbation of the network of hydrogen bonds by the resonant CW laser excitation.

5. Discussion

The photoinduced changes of the optical absorption and the refractive index of KDP:TiO$_2$ SCs can be associated with the resonant excitation of intrinsic defect states of the crystalline matrix and TiO$_2$ NPs surface states. The most important factor of the defect formation mechanism in KDP SCs is the radiation-induced displacement of a proton from its normal site [20]. UV or visible light irradiation can cause the breaking of O-H$\cdots$O bonds, and the diffusion of hydrogen atoms in the crystal lattice can occur. This mechanism is responsible for the transient optical absorption of the crystal at room temperature [12], which was experimentally confirmed in [13, 21]. Within the model, the formation of absorption centers occurs as follows: a proton captures an electron and becomes a neutral hydrogen atom H^0, which moves to the interstitial position due to the thermal diffusion. The oxygen atom closest to the formed hydrogen vacancy captures a hole and forms the radical [HPO$_4$]$^-$ (A-radical). The formation of an autolocalized hole center [H$_2$PO$_4$]^0 (B-radical) is also possible.

The photoinduced changes of optical absorption in the KDP:TiO$_2$ SCs are negligible (Fig. 2). The processes are stationary under the CW laser radiation. Some mechanisms are compensated by others, and, therefore, the NLO changes of optical absorption are weak. At the same time, there are the significant changes of the on-axis transmittance (Figs. 3 and 4), corresponding to refractive index variations. The presence of the resonant excitation of defect states by quanta of light with an energy of ~ 2.3 eV causes the low threshold refractive NLO response at the 532 nm. Effective changes in the refractive index therewith are $\Delta n \sim 10^{-5}$.

Anatase NPs can change the concentration of defects in the KDP:TiO$_2$ SCs due to redox processes on their surface. At the resonant excitation of surface defect states, an electron can be trapped on the NP interface [17]. The further impact on the matrix structure may follow such mechanisms: 1) electrons on the surface of NPs can attract the proton from an O–H$\cdots$O bond; 2) a proton can capture an electron and, after transforming to a neutral hydrogen atom H^0, can shift to the interstitial region. Such nonlocal rearrangement of crystalline matrix hydrogen bonds may change the sign and the magnitude of the refractive NLO response of KDP:TiO$_2$ SCs relatively to the KDP crystal one.

The different impact of anatase NPs on the sign of the NLO refractive response in the prismatic and pyramidal sectors can be explained by various orientations of the growth layers with the incorporated NPs toward to the optical crystal axis – parallel and tilted in the Pr and P series, respectively. For the studied Z-cut Pr samples, the self-focusing effect was observed due to the $\Delta n > 0$ variation in the layers with incorporated NPs. On the contrary, in the P samples, this variation causes a phase contrast enhancement of the tilted layers and a broadening of the beam, which corresponds to the self-defocusing effect in the whole composite material. The proposed explanation is proved by the study of the scattering indicatrix and extinction losses in the samples at 532 nm under the same excitation conditions [19]. The scattering losses in the P samples monotonically increase with the NPs concentration in the matrix. We have observed a scattering losses reduction in Pr-4 in comparison with Pr-5 and Pr-3 samples under resonant excitation conditions. At the He-Ne laser excitation at 633 nm, the NPs incorporation enhances the scattering effect.

Thus, it is shown that the photoinduced variation Δn in KDP and KDP:TiO$_2$ SCs strongly depends on the intrinsic defects concentration in the SC matrix, the crystal growth sector, and the concentration of incorporated anatase NPs under the resonant excitation with the CW laser radiation. The observed phenomenon gives a possibility to monitor the intrinsic defects and the incorporated NPs subsystems in the novel composite material in order to predict its laser-induced damage threshold.

The less efficient non-resonant NLO response at 1064 nm can be applied to the study of the diffusion transport of protons and vacancies in the crystalline matrix by the optical technique.

6. Conclusions

For the first time, the concentration dependence of the cubic nonlinear optical response for different growth sectors of KDP single crystals with incorporated TiO$_2$ nanoparticles (anatase modification) under the CW laser excitation at 532 and 1064 nm is studied. It is shown that the minor photoinduced changes of the optical absorption take place in the crystals with typical values

of the imaginary part of the NLO cubic susceptibility $\mathrm{Im}(\chi^{(3)}) \sim 10^{-7}$ esu.

The TiO$_2$ nanocrystals incorporation changes the sign of the refractive NLO response of the composite system at 532 nm. In the pyramidal growth sector, the self-focusing effect in KDP changes to the self-defocusing in KDP:TiO$_2$. On the contrary, in the prismatic one, the self-defocusing in the crystal matrix turns into the self-focusing in crystals with TiO$_2$ nanoparticles. This fact can indicate the resonant interaction of the subsystem of nanoparticles with intrinsic defects of the crystal matrix. At 1064 nm, the incorporation of nanocrystals changes the refractive NLO response. We propose to apply the effect to monitoring the intrinsic defects and the incorporated NPs subsystems in the KDP-family materials in order to control their laser-induced damage threshold.

The obtained data give a possibility to develop an approach to the control over the phase matching conditions of the second harmonic generation process in KDP and KDP:TiO$_2$ crystals with the additional CW laser irradiation of a crystal at a wavelength of 532 nm. The photoinduced refractive index variation $\Delta n \sim 10^{-5}$ at moderate laser intensities can shift the tuning curves of the generation wavelength by up to 10 nm. The magnitude of the tuning effect depends on the laser radiation intensity, the growth sector of the crystal matrix, and the concentration of incorporated anatase nanoparticles.

1. B. Kahr and R.W. Gurney, Chem. Rev. **101**, 893 (2001).

2. K.L. Wustholz, B. Kahr, and P.J. Reid, J. Phys. Chem. B **109**, 16357 (2005).

3. S.K. Kushwaha, Mohd. Shakir, K.K. Maurya et al., J. Appl. Phys. **108**, 033506 (2010).

4. F. Ben Brahim and A. Buloub, Mater. Chem. Phys. **130**, 24 (2011).

5. P. Kumaresan, S.M. Babu, and P.M. Anbarasan, J. Cryst. Growth **310**, 1999 (2008).

6. J. Podder, J. Crystal Growth **237**, 70 (2002).

7. I. Pritula, V. Gayvoronsky, M. Kopylovsky et al., Funct. Mater. **3**, 420 (2008).

8. I. Pritula, V. Gayvoronsky, M. Kolybaeva et al. Opt. Mat. **33**, 623 (2011).

9. G. Duchateau, G. Geoffroy, A. Dyan et al., Phys. Rev. B **83**, 075114 (2011).

10. C.W. Carr, H.B. Radousky, A.M. Rubenchik et al., Phys. Rev. Lett. **92**, 087401 (2004).

11. S. Demos, R. Negres, P. Demange et al., Opt. Express **18**, 13788 (2010).

12. J. Davis, R. Hughes, and H. Lee, Chem. Phys. Lett. **207**, 540 (1993).

13. I. Ogorodnikov, V. Yakovlev, B. Shul'gin et al., Phys. Solid State **44**, 845 (2002).

14. N. Garces, K. Stevens, S. Demos et al., J. Appl. Phys. **89**, 47 (2001).

15. V.Ya. Gayvoronsky, S.V. Yakunin, V.M. Pergamenshchik et al., Laser Phys. Lett. **3**, 531 (2006).

16. V. Gayvoronsky, S. Yakunin, V. Nazarenko et al., Mol. Cryst. Liq. Cryst. **426**, 231 (2005).

17. V. Gayvoronsky, A. Galas, E. Shepelyavyy et al., Appl. Phys. B **80**, 97 (2005).

18. D.L. Griscom, E.J. Friebele, K.J. Long et al., J. Appl. Phys. **54**, 3743 (1983).

19. V. Gayvoronsky, V. Starkov, M. Kopylovsky et al., Ukr. J. Phys. **55**, 876 (2010).

20. C.S. Liu, Q. Zhang, N. Kioussis et al., Phys. Rev. B **68**, 224107 (2003).

21. S.D. Setzler, K.T. Stevens, M. Yan et al., Phys. Rev. B **57**, 2643 (1998).

ФОТОІНДУКОВАНІ ЗМІНИ ПОКАЗНИКА ЗАЛОМЛЕННЯ МОНОКРИСТАЛІВ KDP З ІНКОРПОРОВАНИМИ НАНОЧАСТИНКАМИ TiO$_2$ ПРИ НЕПЕРЕРВНОМУ ЛАЗЕРНОМУ ЗБУДЖЕННІ

В.Я. Гайворонський, М.А. Копиловський, В.О. Яцина, А.І. Ростоцький, М.С. Бродин, І.М. Притула

Р е з ю м е

Вперше досліджено вплив нанокристалів діоксиду титану у модифікації анатазу на фотоіндуковані зміни оптичного поглинання та показника заломлення монокристалів KDP при самовпливі неперервного лазерного випромінювання на довжинах хвиль 532 і 1064 нм. Показано, що інкорпорування наночастинок анатазу змінює знак рефрактивного нелінійно-оптичного відгуку порівняно з відгуком матриці кристала KDP на довжині хвилі 532 нм внаслідок резонансного перекриття енергетичних положень власних дефектних станів матриці і поверхневих станів наночастинок TiO$_2$. Знак і величина фотоіндукованих змін залежать від концентрації інкорпорованих наночастинок, сектора росту кристала та довжини хвилі лазерного випромінювання.